A HIGH STEP UP DC-DC CONVERET WITH PV CELL FOR DISTRIBUTED GENERATION SYSTEM

Y.Mrudula
PG student,
Dept of EEE SVEC AP.INDIA

B.Subbareddy,
Assistant professor
Dept of EEE, SVEC A.P,India.

T.Devaraju,
HOD Dept of EEE, P.Hd
SVEC A.P, India.

Abstract

During the first decade of the 21st century, the world wide photovoltaic (PV) markets have experienced a tremendous expansion. One reason for installing distributed generation in general of which distributed PV is a special case is to locate power generation closer to the load. A high step-up converter with PV cell for a distribution generation system is this paper. The concept is combined of two capacitors, two diodes and one coupled inductor and photovoltaic cell. Two capacitors are charged in parallel and are discharged in series by the coupled inductor. The high step up voltage gain can be get with an appropriate duty ratio. The voltage stresses on the main switch and output diode are reduced by a passive clamp circuit. Therefore, low resistance RDS(ON) for the main switch can be adopted to reduce conduction loss. In addition, the reverse recovery problem of the diode is alleviated and thus, the efficiency can be further improved. The operating principle and steady-state analyses of the voltage gain are also discussed in detail. Finally, a 24volts input voltage, 400volts output voltage and 400Watts output power prototype circuit of the proposed converter are implemented in the simulink to verify the performance.

Keywords **- PV system, IGBT ,distributed generation system, high stepup dc-dc converter, coupled inductors**

I. INTRODUCTION

In a micro grid system, all system components such as battery inverter, diesel generator, PV solar array, wind-turbine, hydro-turbine etc. are connected together via the ac-network [1-5]. This allows these components to be placed on any location on the property and also allows for easy expansion of the system. A system can start as a simple 5kW single phase stand alone system and grow into a large 3-phase network with multiple houses, multiple PV arrays and multiple wind-turbines connected. Micro grid systems are used as stand-alone power systems or as distributed generation systems that are connected to the public grid at one common point. These distributed generation systems can be a cost effective solution for sub-divisions with limited capacity from the public grid. Fig.1 shows a photovoltaic distributed system have the solar energy source is low dc input voltage. Photovoltaic sources are connected in series to produce a sufficient dc voltage for generating ac utility voltage. However it is difficult to realize a series connection of the photovoltaic source without incurring a shadow effect [6-7]. The photovoltaic source produce very low voltage, I want high dc voltage, we are using high step up dc-dc converters. The low voltage (12-14V) to high voltage(380-400V)[8]. The high step up dc-dc converters wanted high conversion ratio, high efficiency and small size [9-14]. The dc-dc converters are two types. They are isolated and non-isolated dc-dc converters. The non-isolated dc-dc converters are buck, boost, buck-boost. These are low voltage gain are produces. But any time fault occurs on the load side directly effects on the supply side, finally the system will collapse. So we are going to the isolated converters. They are fly back, forward, push-pull, sepic, cuk converters. These are high step-up voltage gain produced by adjusting the transformer windings. However,

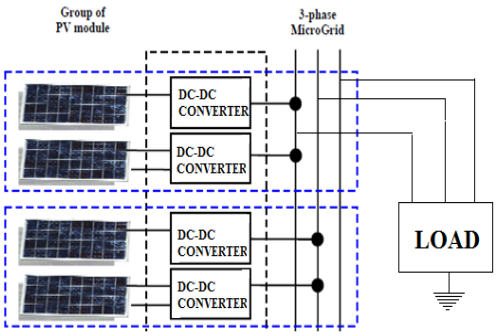

Figure. 1 Photovoltaic distributed system

the main switches of these converters are suffering a heavy voltage spike and high power loss from the leakage inductor of the transformer [15]. To decrease these disadvantages, the nondissipative snubber circuits and active clamp circuits are employed. However the cost increases accordingly due to the extra power switch and high side driver[16].

Theoretically, the non isolated converters can be added to provide high step-up voltage gain with extremely high duty cycle [17]. However, the step-up voltage gain certain range by the effect of the semiconductor switches, rectifier diodes and equivalent series resistance of the inductors and capacitors. The extreme duty cycle operation may also result in serious reverse-recovery problem and electromagnetic interference problem [18].

To improve the conversion efficiency and get high step-up voltage gain, much topography has been proposed [17-26].

High step-up gain can be gained by the use of the switched capacitor technique [20-23].A coupled inductor is used in a boost or buck-boost converter instead of the input inductor. However, the main switch will suffering high transient current and conduction loss is high. Another method for achieving high step-up gain is the use of the voltage-lift technique [24-26]. However, it is the same disadvantage. The converters designing the coupled-inductor technique to get high step-up gain by adjusting the turns ratio[27].

The system analysis, design consideration, and implementation of a soft-switching zeta-fly back converter to achieve zero-voltage switching (ZVS). In proposed converter the zeta and flyback topologies are adopted in the output side to achieve the following features: to share the power components in the transformer primary side, to achieve the partial magnetizing flux reset, and to share the output power .The buck-boost type of active clamp is connected in parallel with the primary side of the isolation transformer to recycle the energy stored in the leakage inductor of isolated transformer and to limit the peak voltage stress of switching devices due to the transformer leakage inductor when the main switch is turned off. The active clamp circuit can make the switching devices to turn on at ZVS [28-29].An integrated boost-fly back converter is presented, in which the secondary side of the coupled inductor is used as a flyback-type[30-31]. The proposed converter topology can promote the voltage gain of a conventional boost converter with a single inductor, and deal with the problem of the leakage inductor and demagnetization of transformer for a coupled-inductor-based converter [32-34].A new type of non-isolated step-up converter with high voltage gain is proposed on this work. It is suitable for applications with a high voltage gain between the input and the output stages. In this converter, the output to input voltage ratio, for a given duty cycle, can be raised by adding voltage multiplier stages of capacitors (mc) [35-36].The sepic-fly back converter with the coupled inductor and output stacking techniques has been proposed [37]. Additionally, a high step-up boost converter that uses multiple coupled inductors with output stacking has been proposed [38-39].

A special type of power FET that has the function of a BJT with its base driven by a FET. Faster than a BJT of similar ratings, and easy to use. Ratings from 10 to >600 A, with voltages of 600 to 1700V. The IGBT is popular in inverters from 1 to 100kW or more. It is found almost exclusively in power electronics applications.

This paper proposes a high efficiency, high step-up voltage gain, and clamp-mode converter. The proposed converter adds two pairs of additional capacitors and diodes to achieve high step-up voltage gain. The coupled inductor is used as both a forward and flyback type; thus, the two capacitors can be charged in parallel and discharged in series via the coupled inductor. The transit current does not flow through the main switch compared with earlier studies [20–26]. Thus, the proposed converter has low conduction loss. Additionally, this converter allows significant weight and volume reduction compared with other converters [27–[38]. Another benefit is that the voltage stresses on the main switch and output diode are reduced. However, the leakage inductor of the coupled inductor may cause high power loss and voltage spike. Thus, a passive clamping circuit is needed to recycle the leakage-inductor energy of the coupled inductor and to clamp the voltage across the main switch. The reverse-recovery problems in the diodes are alleviated, and thus, high efficiency can be achieved.

II.OPERATION FOR THE DC-DC PROPOSED CONVERTER

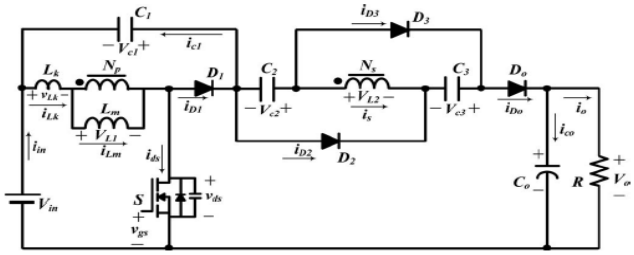

Figure 2: Circuit of proposed converter

Fig. 2 shows the circuit topology of the proposed converter. This converter consists of PV cell as input source consists of modeling of PV cells power switch *S*, coupled inductors *Np* and *Ns*, one clamp diode *D*1, clamp capacitor *C*1, two blocking capacitors *C*2 and *C*3, two blocking diodes *D*2 and *D*3, output diode *Do*, and output capacitor *Co*. The coupled inductor is modeled as the magnetizing inductor *Lm* and leakage inductor *Lk* .Fig 3 shows the example of the circuit analysis with dc as input source

To simplify the circuit analysis, the following conditions are assumed.

1) Capacitors *C*2 , *C*3 , and *Co* are large enough that *Vc* 2, *Vc* 3 and *Vo* are considered to be constant in one switching period.

2) The power MOSFET and diodes are treated as ideal, but the parasitic capacitor of the power switch is considered

3) The coupling coefficient of coupled inductor *k* is equalto *Lm*/(*Lm*+*Lk*) and the turns ratio of coupled inductor *n* is equal to *Ns* /*Np* period.

A. Continuous-Conduction Mode (CCM) Operation

In CCM operation, there are six operating modes in one switching period of the proposed converter. Fig.

4shows the typical waveforms and Fig. 5 shows the current-flow path of the proposed converter for each modes. The operating modes are described as follows.

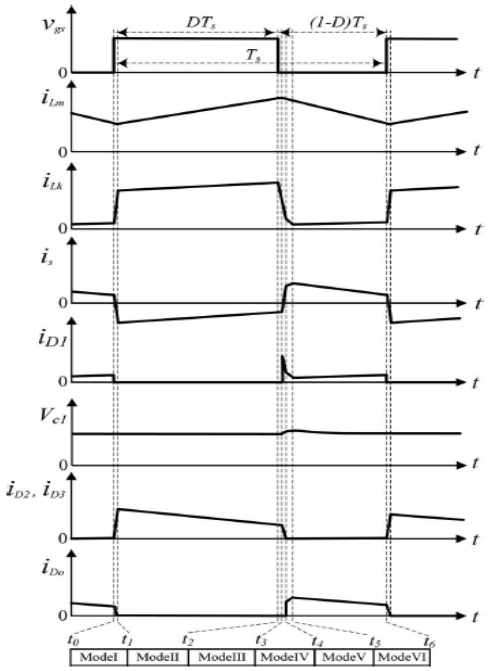

Figure.4 The waveforms of the proposed converter operation in CCM

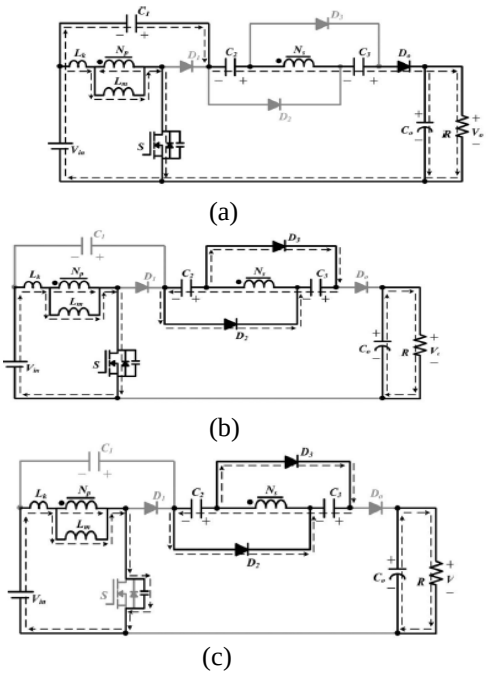

(a)

(b)

(c)

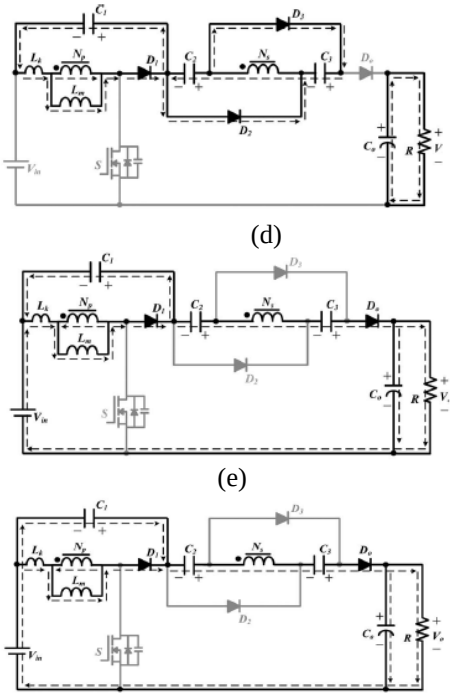

(d)

(e)

(f)

Figure.5 In CCM operation the current flowing in operating modes (a) Mode I (b) Mode II (c) Mode III (d) Mode IV (e)Mode V (f) Mode VI

1) *Mode* I [*t*0, *t*1]: During this time interval, *S* is turned on. Diodes *D*1, *D*2, and *D*3 are turned off, and *Do* is turned on. The current-flow path is shown in Fig. 5(a). The primary-side current of the coupled inductor *iLk* is increased linearly. The magnetizing inductor *Lm* stores its energy from dc source *V*in. Due to the leakage inductor *Lk* , the secondary-side current of the coupled inductor *I s* is decreased linearly. The voltage across the secondary side winding of the coupled inductor *VL* 2 , and blocking voltages *Vc*2 and *Vc*3 are connected in series to charge the output capacitor *Co* and to provide the energy to the load *R*. When the current *is* becomes zero, dc source *V*in begins to charge capacitors *C*2 and *C*3 via the coupled inductor. When *iLk* is equal to *iLm* at $t = t1$ this operating mode ends.

2) *Mode* II [*t*1, *t*2]: During this time interval, *S* is still turned On. Diodes *D*1 and *Do* are turned off, and *D*2 and *D*3 are turned on. The current-flow path is shown in Fig. 5(b). The magnetizing inductor *Lm* is stored energy from dc source *V*in Some of the energy from dc source *V*in transfers to the secondary side of the coupled inductor to charge the capacitors *C*2 and *C*3. Voltages *Vc*2 and *Vc*3 are approximately equal to *nV*in. Output capacitor *Co* provides the energy to load *R*. This operating mode ends when switch *S* is turned off at $t = t2$.

3) *Mode* III [*t*2, *t*3]: During this time interval, *S* is turned off. Diodes *D*1 and *Do* are turned off, and *D*2 and *D*3 are turned on. The current-flow path is shown in Fig. 5(c). The

energies of leakage inductor *Lk* and magnetizing inductor *Lm* are released to the parasitic capacitor *C*ds of switch *S*. The capacitors *C*2 and *C*3 are still charged by the dc source *V*in via the coupled inductor. The output capacitor *Co* provides energy to load *R*. When the capacitor voltage *V*in+*V*ds is equal to *Vc*1 at $t = t3$, diode *D*1 conducts and this operating mode ends.

4) *Mode* IV [*t*3, *t*4]: During this time interval, *S* is turned off. Diodes *D*1, *D*2, and *D*3 are turned on and *Do* is turned off. The current-flow path is shown in Fig. 5(d). The energies of leakage inductor *Lk* and magnetizing inductor *Lm* are released to the clamp capacitor *C*1. Some of the energy stored in *Lm* starts to release to capacitors *C*2 and *C*3 in parallel via the coupled inductor until secondary current *is* equals to zero. Meanwhile, current *iLk* is decreased quickly. Thus, diodes *D*2 and *D*3 are cut off at $t = t4$, and this operating mode ends.

5) *Mode* V [*t*4 , *t*5]: During this time interval, *S* is turned off. Diodes *D*1 and *Do* are turned on, and *D*2 and *D*3 are turned off. The current-flow path is shown in Fig. 5(e). The energies of leakage inductor *Lk* and magnetizing inductor *Lm* are released to the clamp capacitor *C*1. The primary and secondary windings of the coupled inductor, dc sources *V*in, and capacitors *C*2 and *C*3 are in series to transfer their energies to the output capacitor *Co* and load *R*. This operating mode ends when capacitor *C*1 starts to discharge at $t = t5$.

6) *Mode* VI [*t*5, *t*6]: During this time interval, *S* is still turned off. Diodes *D*1 and *Do* are turned on, and *D*2 and *D*3 are turned off. The current-flow path is shown in Fig. 5(f). The primary-side and secondary-side windings of the coupled inductor, dc sources *V*in, and capacitors, *C*1, *C*2, and *C*3, transfer their energies to the output capacitor *Co* and load *R*. This mode ends at $t = t6$ when *S* is turned on at the beginning of the next switching period.

B. Discontinuous-Conduction Mode (DCM) Operation

In order to simplify the analysis for DCM operation, leakage inductor *Lk* of the coupled inductor is neglected. Fig. 6 shows the typical waveforms when the proposed converter is operated in DCM, and Fig. 7 shows the current-flow path of the proposed converter for each mode. There are three modes in DCM operation. The operating modes are described as follows.

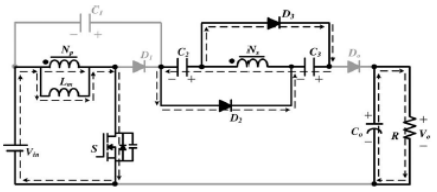

(a)

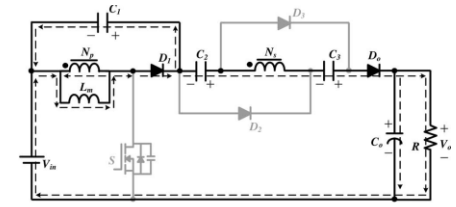

(b)

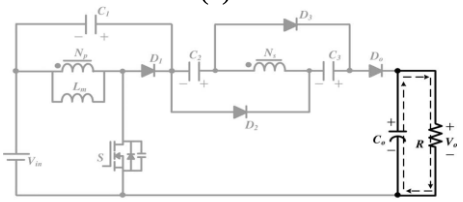

(c)

Figure .6 In DCM operation the current flowing in operating modes (a) Mode I (b) Mode II (c) Mode III

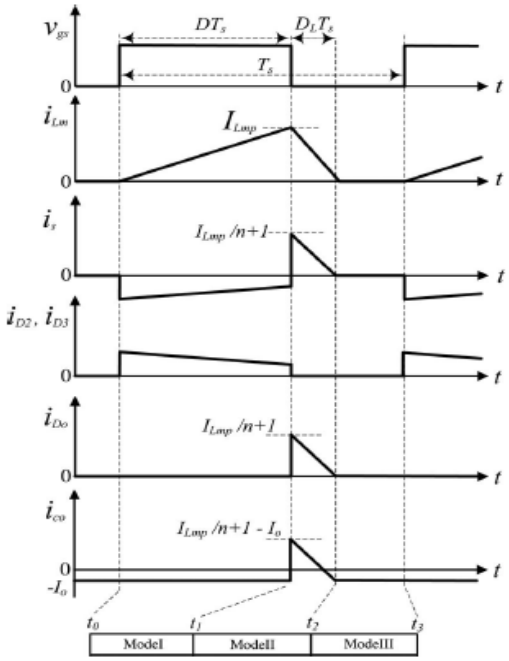

Fig.6 The wave forms of the proposed converter in DCM

1) Mode I [t0, t1]: During this time interval, S is turned on. The current-flow path is shown in Fig. 7(a). The part energy of dc source Vin transfers to magnetizing inductor Lm. Thus, iLm is increased linearly. The dc source Vin also transfers another part energy to charge capacitors C2 and C3 via the coupled inductor. The energy of the output capacitor Co is discharged to load R. This mode ends when S is turned off at t = t1.

2) *Mode* II [*t*1, *t*2]: During this time interval, *S* is turned off. The current-flow path is shown in Fig. 7(b). The energy of the magnetizing inductor *Lm* is released to the capacitor *C*1. Similarly, capacitors *C*2 and *C*3 are discharged in a series with dc source *V*in and magnetizing inductor *Lm* to the capacitor *Co* and load *R*. This mode ends when the energy stored in *Lm* is depleted at *t* = *t*2.

3) *Mode* III [*t*2, *t*3]: During this time interval, *S* remains turned off. The current-flow path is shown in Fig. 7(c). Since the energy stored in *Lm* is depleted, the energy stored in *Co* is discharged to load *R*. This mode ends when *S* is turned on at *t* = *t*3.

II. STEADY-STATE ANALYSIS OF THE DC-DC CONVERTER

A. CCM Operation

At modes IV and V, the energy of the leakage inductor *Lk* is released to the clamped capacitor *C*1 . According to previous work [13], the duty cycle of the released energy can be expressed as

$$D_{c1} = \qquad (1)$$

where *Ts* is the switching period, *Dc* 1 is the duty ratio of the switch, and *tc* 1 is the time of modes IV and V. By applying the voltage-second balance principle on *Lm*, the voltage across the capacitor *C*1 can be represented by

$$V_{c1} = \frac{D}{1-D}.V_{in}.\frac{(1+k)+}{} \qquad (2)$$

Since the time durations of modes I, III, and IV are significantly short, only modes II, V, and VI are considered in CCM operation for the steady-state analysis.

In the time period of mode II, the following equations can be written based on Fig.5(b):

$$v_{L1}^{II} = \frac{L_m}{L_m+L_{k1}}V_i \qquad (3)$$

$$v_{L2}^{II} = nv_{L1}^{II} \qquad (4)$$

Thus, the voltage across capacitors *C*2 and *C*3 can be written As

$$V_{c2} = V_c \qquad (5)$$

During the time duration of modes V and VI, the following equation can be formulated based on Fig.5(f):

$$v_{L2}^{V} = v_{L2}^{VI} = V_{in} + V_{c1} + V_{c2} + \qquad (6)$$

Thus, the voltage across the magnetizing inductor *Lm* can be derived as

$$v_{L1}^{V} = v_{L1}^{VI} = \frac{v_{L2}^{VI}}{n} = \frac{V_{in}+V_{c1}+V_c}{n} \qquad (7)$$

Using the volt-second balance principle on *Lm*, the following equation is given:

$$\int_0^{DT_s} v_{L1}^{II} + \int_{DT_s}^{T_s} v_{L1}^{VI} = 0 \qquad (8)$$

Substituting (2), (3), (5), and (7) into (8), the voltage gain is

Obtained as

$$M_{CCM} = \frac{1+nk}{1-D} + nk + \frac{D}{1-D}.\frac{(1-k)}{} \qquad (9)$$

The schematic of the voltage gain versus the duty ratio under various coupling coefficients of the coupled inductor is shown in Fig. 9. It is seen that the voltage gain is not very sensitive to the coupling coefficient. When *k* is equal to 1, the ideal voltage gain is written as Fig. 9 shows the voltage gain versus the duty ratio of the proposed converter as compared with the converters in previous work [33] and [34] at CCM operation under *k* = 1 and *n* = 3. One can see that the voltage gain of the proposed converter is higher than those of the converters in [33] and [34]. According to the description of the operating modes, the voltage stresses on the active switch *S* and diodes *D*1,*D*2, *D*3 , and *Do* are given as

N (10)

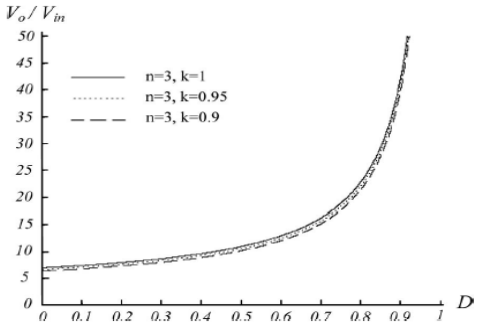

Figure. 8. Voltage gain versus duty ratio at CCM operation under *n = 3 and* various *k*.

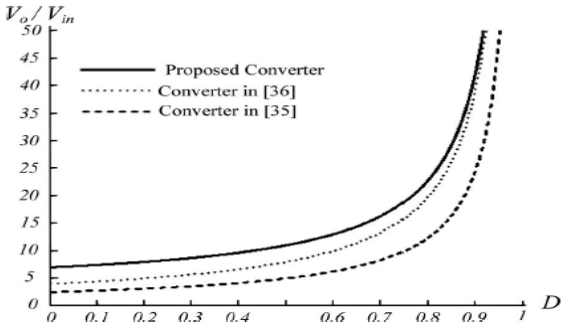

Figure. 9. Voltage gain versus duty ratio of the proposed converter, the converters in [33] and [35] at CCM operation under *n* = 3 and *k* = 1.

$$V_{DS} = \frac{1}{1-D}V_{in} \qquad (11)$$

$$V_{D1} = \frac{1}{1-D}V_{in} = \frac{V_0-nV_{in}}{n+1} \qquad (12)$$

$$V_{D2} = V_{D3} = V_{D0} = \frac{n}{1-D}V_{in} = \frac{n}{n+1}\ V_0 - nV_{in} \qquad (13)$$

Equations (11)–(13) mean that with the same specifications, the voltage stresses on the main switch and diodes can be adjusted by the turns ratio of the coupled inductor.

B. DCM Operation

In DCM operation, three modes are discussed. The key waveform is shown in Fig. 7. During the time of mode I,

the switch *S* is turned on. Thus, the following equations can be formulated based on Fig. 7(a):

(14)

(15)

The peak value of the magnetizing inductor current is given
as

(16)

Furthermore, the voltage across capacitors *C*2 and *C*3 can be
written as

$$V_{c2} = V_{c3} = v_{L2}^{I} = \quad (17)$$

In the time interval of mode II, the following equations can
be expressed based on Fig. 6(b):

$$v_{L1}^{II} = \cdot \quad (18)$$

$$v_{L2}^{II} = V_{in} + V_{c1} + V_{c2} \quad (19)$$

During the time of mode III, the following equation can be derived from Fig. 6(c):

$$v_{L1}^{III} = v_{L2}^{III} : \quad (20)$$

Applying the voltage-second balance principle on *Np* , *Ns* of
the coupled inductor, the following equations are given as

$$\int_0^{DT_s} v_{L1}^{I}\,dt + \int_{DT_s}^{(D+D_L)T_s} v_{L1}^{II}\,dt + \int_{(D+D_L)T_s}^{T_s} v_{L1}^{III}\,dt = \quad (21)$$

$$\int_0^{DT_s} v_{L2}^{I}\,dt + \int_{DT_s}^{(D+D_L)T_s} v_{L2}^{II}\,dt + \int_{(D+D_L)T_s}^{T_s} v_{L2}^{III}\,dt = 0 \quad (22)$$

Substituting (14), (15), (17), (18), (19), and (20) into (21) and (22), the voltage gain is obtained as follows:

$$V_{c1} = \frac{D}{D_L} V_{in} \quad (23)$$

$$V_{c1} = \left[\frac{D}{D_L}(n+1) + (2n + \right. \quad (24)$$

According to (24), the duty cycle *DL* can be derived as

$$D_L = \frac{(1+n)DV_{in}}{V_0 - (1+2n)V_{in}} \quad (25)$$

From Fig. 5, the average current of *i*co is computed as

$$I_{c0} = \frac{1}{2} D_L \frac{I_{Lmp}}{n+1} \cdot \quad (26)$$

Since *I*co is equal to zero under steady state, (16), (25), and
*I*co = 0 into (26) yield

$$\frac{I}{2[V_0 -} \quad (27)$$

Then, the normalized magnetizing-inductor time constant is
defined as

$$\tau_{Lm} \equiv \frac{}{} \quad (28)$$

where *fs* is the switching frequency.
Substituting (28) into (27), the voltage gain is given by

$$M_{DCM} = \frac{V_0}{V_{in}} = \frac{1+2n}{2} + \sqrt{\frac{(1+2n)}{4} + \frac{D^2}{2\tau_{Lm}}} \quad (29)$$

The curve of the voltage gain, shown in Fig. 9, illustrates the voltage gain versus the duty ratio under various *τLm*.

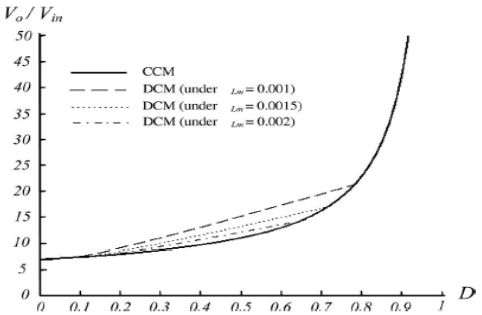

Figure. 10. Voltage gain versus duty ratio at DCM operation under various *τLm*and at CCM operation under *n* = 3 and *k* = 1.

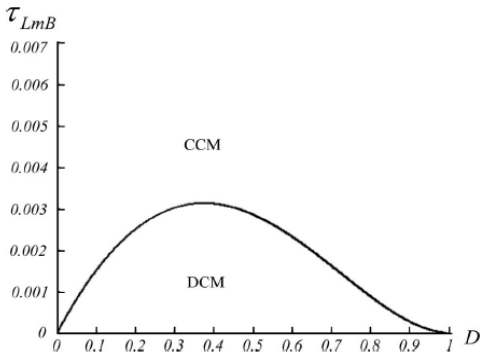

Figure. 11. Boundary condition of the proposed converter under *n* = 3.

C. Boundary Operating Condition Between CCM and DCM

If the proposed converter is operated in boundary-condition mode, the voltage gain of CCM operation is equal to the voltage gain of DCM operation. From (10) and (29), the boundary normalized magnetizing-inductor time constant *τLmB* can be derived as Applying the voltage-second balance principle on *Np*, *Ns* of the coupled inductor, the following equations are given as

$$\tau_{LmB} \quad (30)$$

The curve of *τLmB* is plotted in Fig. 11. If *τLm* is larger than
τLmB , the proposed converter is operated in CCM.

IV MATLAB/SIMULINK MODELING AND SIMULATION RESULTS

A simulation modeling of a PV distributed system with high step up dc dc converter is showed bellow-

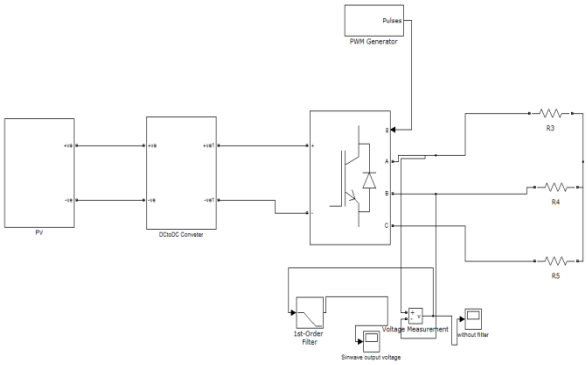

Figure 12. Simulink modeling of PV distributed system

PV connect in series to DC-DC converter obtain sufficient dc voltage for generating ac utility voltage. IGBT which is connected to the load .PWM generator generates the pulse to the diode .The internal structure of the DC-DC converter as shown below

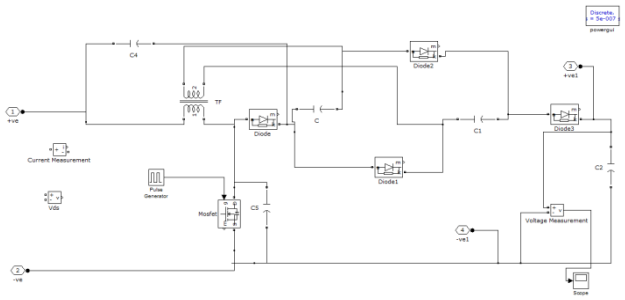

Figure13:Internal structure of the DC-DC converter

Fig 13 shows the internal structure of the dc-dc converter with input as photovoltaic cell of voltage of(15V-17V)and getting output of 240v .The below fig shows the ouptput of the dc-dc conveter

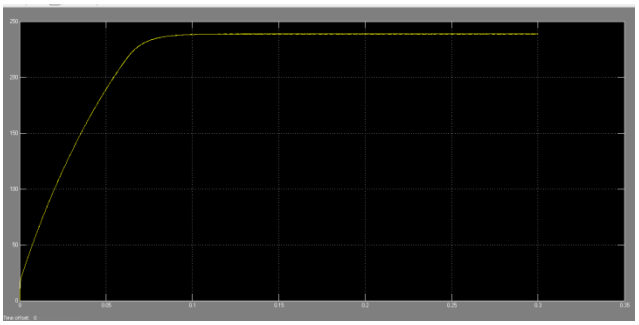

Figure 14: Output response of the DC-DC converter

The Fig 14 shows that the output response of the dc-dc converter With 240V . The IGBT which is a special type of power FET that has the function of a BJT with its base driven by a FET. Faster than a BJT of similar ratings, and easy to use. Ratings from 10 to >600 A, with voltages of 600 to 1700V. The IGBT is popular in inverters from 1 to 100kW or more. It is found almost exclusively in power electronics applications Focusing on PV systems, a typical "12 Volt" PV module or panel has 36 series connected solar cells with a maximum power point (MPP) of approximately 15V at normal operating temperatures (approx 50°C). These system voltages are appropriate for lower power systems, but beyond powers of a few hundred Watts, these panels themselves are placed in series strings PV arrays to maintain lower currents and higher efficiencies.

A problem occurs when even a single cell in the array is shaded or obscured. The photocurrent generated in a shaded cell may drop to perhaps 20% of the other cells. The shaded cell will be reverse biased by the remaining cells in the string, but current will continue to flow through it causing large localized power dissipation.

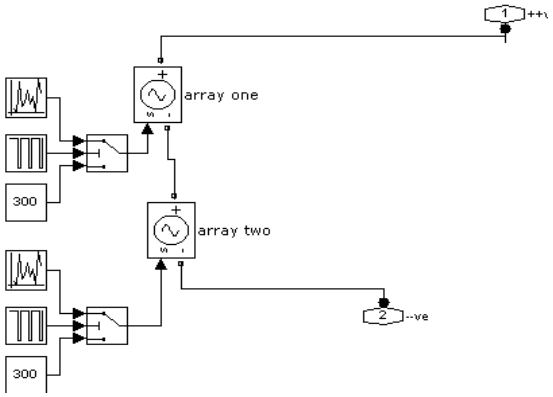

Figure 15: Modeling of solar array

The overall efficiency of the array is reduced to the efficiency of this module. For similar reasons PV panels in a string should be given the same orientation, and be of identical size. This is not always possible or desirable for ascetic or other architectural reasons.

The first order filter output sinwave voltage used in the simulink model of the proposed circuit is shown in the below wave form of the PV distributed system

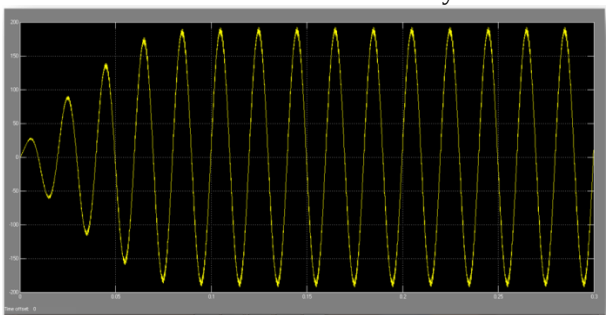

Figure 17: Response of the PV distributed system with filter

Fig 17 shows that the output response of the PV distributed system using the filter we get the sinusoidal output voltage as shown

VI CONCLUSION

This paper proposed a high gain and high efficiency using PV cell for a distributed system. By using the PV cell in series and discharged in a series to the Dc-Dc converter to

achieve high step-up voltage gain and high efficiency. The steady-state analyses of voltage gain and boundary operating condition are discussed in detail. Prototype circuit of the proposed converter is built in the laboratory. Experimental results confirm that high efficiency and high step-up voltage gain can be achieved. The efficiency is 95.5%. The voltage stress on the main switches is 90 V; thus, low voltage ratings and low on-state resistance levels *R*DS(ON) switch can be selected. Moreover, the proposed converter has simple structure. It is suitable for renewable energy systems for the distributed generation system applications.

VII REFERENCES

[1] C. L. Chen, Y. W, J. S. Lai, Y. S. Lee, and D. Martin, "Design of parallel inverters for smooth mode transfer microgrid applications," *IEEE Trans.Power Electron.*, vol. 25, no. 1, pp. 6–15, Jan. 2010.

[2] A. Timbus, M. Liserre, R. Teodorescu, P. Rodriguez, and F. Blaabjerg, "Evaluation of current controllers for distributed power generation systems," *IEEE Trans. Power Electron.*, vol. 24, no. 3, pp. 654–664, Mar. 2009.

[3] Y. A.-R. I. Mohamed and E. F. El Saadany, "Hybrid variable-structure control with evolutionary optimum-tuning algorithm for fast grid-voltage regulation using inverter-based distributed generation," *IEEE Trans. Power Electron.*, vol. 23, no. 3, pp. 1334–1341, May 2008.

[4] Y. A.-R. I. Mohamed and E. F. El Saadany, "Adaptive decentralized droop controller to preserve power sharing stability of paralleled inverters in distributed generation microgrids," *IEEE Trans. Power Electron.*, vol. 23, no. 6, pp. 2806–2816, Nov. 2008.

[5] Y. W. Li and C. -N. Kao, "An accurate power control strategy for powerelectronics-interfaced distributed generation units operating in a lowvoltagemultibus microgrid," *IEEE Trans. Power Electron.*, vol. 24, no. 12, pp. 2977–2988, Dec. 2009.

[6] H. Karimi, A. Yazdani, and R. Iravani, "Negative-sequence current injection for fast islanding detection of a distributed resource unit," *IEEE Trans. Power Electron.*, vol. 23, no. 1, pp. 298–307, Jan. 2008.

[7] T. Shimizu,K.Wada, andN.Nakamura, "Flyback-type single-phase utility interactive inverter with power pulsation decoupling on the dc input for an ac photovoltaic module system," *IEEE Trans. Power Electron.*, vol. 21, no. 5, pp. 1264–1272, Sep. 2006.

[8] L. Palma, M. H. Todorovic, and P. Enjeti, "A high gain transformerless DC–DC converter for fuel-cell applications," in *Proc. IEEE Power Electron. Spec. Conf. (PESC)*, 2005, pp. 2514–2520.

[9] P. Biczel, "Power electronic converters in dc microgrid," in *Proc. IEEE Compat. Power Electron. Conf. (CPE)*, 2007, pp. 1–6.

[10] A. M. Salamah, S. J. Finney, and B. W. Williams, "Single-phase voltage source inverter with a bidirectional buck–boost stage for harmonic injection and distributed generation," *IEEE Trans. Power Electron.*, vol. 24, no. 2, pp. 376–387, Feb. 2009.

[11] A. Cid-Pastor, L. Martinez-Salamero, C. Alonso, A. El Aroudi, and H.Valderrama-Blavi, "Power distribution based on gyrators," *IEEE Trans. Power Electron.*, vol. 24, no. 12, pp. 2907–2909, Dec. 2009.

[12] L. S.Yang,T. J. Liang, and J. F.Chen, "Transformer-lessDC–DCconverter with high voltage gain," *IEEE Trans. Ind. Electron.*, vol. 56, no. 8, pp. 3144–3152, Aug. 2009.

[13] Q. Zhao and F. C. Lee, "High-efficiency, high step-up dc–dc converters," *IEEE Trans. Power Electron.*, vol. 18, no. 1, pp. 65–73, Jan. 2003.

[14] R. J. Wai, C. Y. Lin, C. Y. Lin, R. Y. Duan, and Y. R. Chang, "Highefficiency power conversion system for kilowatt-level stand-alone generation unit with low input voltage," *IEEE Trans. Ind. Electron.*, vol. 55, no. 10, pp. 3702–3714, Oct. 2008.

[15] N. P. Papanikolaou and E. C. Tatakis, "Active voltage clamp in flyback converters operating in CCM mode under wide load variation," *IEEE Trans. Ind. Electron.*, vol. 51, no. 3, pp. 632–640, Jun. 2004.

[16] J. M. Kwon and B. H. Kwon, "High step-up active-clamp converter with input-current doubler and output-voltage doubler for fuel cell power systems," *IEEE Trans. Power Electron.*, vol. 24, no. 1, pp. 108–115, Jan. 2009.

[17] B. Axelrod, Y. Berkovich, and A. Ioinovici, "Transformerless DC–DC converters with a very high DC line-to-load voltage ratio," in *Proc. IEEE Int. Symp. Circuits Syst. (ISCAS)*, 2003, pp. III435–III438.

[18] R. J. Wai and R. Y. Duan, "High-efficiency DC/DC converter with high voltage gain," *IEE Proc. Inst. Elect. Eng.-Electr. Power Appl.*, vol. 152, no. 4, pp. 793–802, Jul. 2005.

[19] J. A. Carr, D. Hotz, J. C. Balda, H. A. Mantooth, A. Ong, and A. Agarwal,"Assessing the impact of SiC MOSFETs on converter interfaces for distributed energy resources," *IEEE Trans. Power Electron.*, vol. 24, no. 1, pp. 260–270, Jan. 2009.

[20] F. Zhang, L. Du, F. Z. Peng, and Z. Qian, "A new design method for high-power high-efficiency switched-capacitor dc–dc converters," *IEEE Trans. Power Electron.*, vol. 23, no. 2, pp. 832–840, Mar. 2008.

[21] O. Abutbul, A. Gherlitz, Y. Berkovich, and A. Ioinovici, "Step-up switching-mode converter with high voltage gain using a switchedcapacitor circuit," *IEEE Trans. Circuits Syst. I*, vol. 50, no. 8, pp. 1098– 1102, Aug. 2003.

[22] B. Axelrod, Y. Berkovich, and A. Ioinovici, "Switched-capacitor/ switched-inductor structures for getting transformerless hybrid DC–DC PWM converters," *IEEE Trans. Circuits Syst. I*, vol. 55, no. 2, pp. 687– 696, Mar. 2008.

[23] B. Axelrod, Y. Berkovich, and A. Ioinovici, "Switched-capapcitor (SC)/Switched-inductor (SL) structures for getting hybrid step-down CUK/ZETA/SEPIC converters," in *Proc. IEEE Int. Symp. Circuits Syst. (ISCAS)*, 2006, pp. 5063–5066.

[24] F. L. Luo, "Six self-lift DC–DC converters, voltage lift technique," *IEEE Trans. Ind. Electron.*, vol. 48, no. 6, pp. 1268–1272, Dec. 2001. 1136 IEEE TRANSACTIONS ON POWER ELECTRONICS, VOL. 26, NO. 4, APRIL 2011

[25] F. L. Luo and H. Ye, "Positive output super-lift converters," *IEEE Trans.Power Electron.*, vol. 18, no. 1, pp. 105–113, Jan. 2003.

[26] F. L. Luo and H. Ye, "Positive output multiple-lift push–pull switchedcapacitor Luo-converters," *IEEE Trans. Ind. Electron.*, vol. 51, no. 3, pp. 594–602, Jun. 2004.

[27] B. Axelrod, Y. Berkovich, and A. Ioinovici, "Switched coupled inductor cell for DC–DC converters with very large conversion ratio," in *Proc. IEEE IECON Conf.*, 2006, pp. 2366–2371.

[28] B. R. Lin and F. Y. Hsieh, "Soft-switching zeta–flyback converter with a buck–boost type of active clamp," *IEEE Trans. Ind. Electron.*, vol. 54, no. 5, pp. 2813–2822, Oct. 2007.

[29] T. F. Wu, Y. S. Lai, J. C. Hung, and Y. M. Chen, "Boost converter with coupled inductors and buck–boost type of active

clamp," *IEEE Trans. Ind. Electron.*, vol. 55, no. 1, pp. 154–162, Jan. 2008.
[30] K. C. Tseng and T. J. Liang, "Novel high-efficiency step-up converter," *IEE Proc. Inst. Elect. Eng.-Electr. Power Appl.*, vol. 151, no. 2, pp. 182– 190, Mar. 2004.
[31] K. C. Tseng and T. J. Liang, "Analysis of intergrated boost-flyback stepup converter," *IEE Proc. Inst. Elect. Eng.-Electric Power Appl.*, vol. 152, no. 2, pp. 217–225, 2005.
[32] R. J.Wai and R. Y. Duan, "High step-up converter with coupled inductor," *IEEE Trans. Power Electron.*, vol. 20, no. 5, pp. 1025–1035, Sep. 2005.
[33] R. J. Wai, L. W. Liu, and R. Y. Duan, "High-efficiency voltage- clamped DC–DC converter with reduced reverse-recovery current and switchvoltage stress," *IEEE Trans. Ind. Electron.*, vol. 53, no. 1, pp. 272–280, Feb. 2005.
[34] J. W. Baek, M. H. Ryoo, T. J. Kim, D. W. Yoo, and J. S. Kim, "High boost converter using voltage multiplier," in *Proc. IEEE IECON*, 2005, pp. 567–572.
[35] T. Dumrongkittigule, V. Tarateeraseth, and W. Khan-ngern, "A new integrated inductor balanced switching technique for common mode EMI reduction in high step-up DC/DC converter," in *Proc. Int. Zurich Symp. Electromagn. Compat.*, 2006, pp. 541–544.
[36] Y. J. A. Alcazar, R. T. Bascope, D. S. de Oliveira, E. H. P. Andrade, and W. G. Cardenas, "High voltage gain boost converter based on threestate switching cell and voltage multipliers," in *Proc. IEEE IECON*, 2008, pp. 2346–2352.
[37] K. B. Park, H. W. Seong, H. S. Kim, G. W. Moon, and M. J. Youn, "Integrated boost-sepic converter for high step-up applications," in *Proc. Power Electron. Spec. Conf.*, Rohode, Greece, 2008, pp. 944–950.
[38] G. V. T. Bascope, R. P. T. Bascope, D. S. Oliveira, S. A. Vasconcelos,F. L. M. Antunes, and C. G. C. Branco, "A high step-up DC–DC converter based on three-state switching cell," in *Proc. IEEE Int. Soc. Ind. Ecology (ISIE)*, 2006, pp. 998–1003.